

# Measurement of the photoeffect cross section and the K-absorption edge energy of Dy, Ta, Pt and Au atoms using bremsstrahlung

Juan Alejandro García Álvarez<sup>1</sup>, Neivy López Pino<sup>1</sup>, Oscar Díaz Rizo<sup>1</sup>, Yasser Corrales<sup>1</sup>, Fátima Padilla Cabal<sup>1</sup>, Maily Pérez Liva<sup>1</sup>, Katia D'Alessandro<sup>1</sup>, Nora L. Maidana<sup>2</sup>

<sup>1</sup>Departamento de Física Nuclear. Instituto Superior de Tecnologías y Ciencias Aplicadas (InSTEC)  
Ave. Salvador Allende esq. Luaces, Quinta de los Molinos. La Habana, Cuba

<sup>2</sup>Laboratório do Acelerador Linear, Instituto de Física da USP, Rua do Matao, Travessa R., 187, 05508-900, SP, Brazil  
jagarcia@instec.cu

## Abstract

An experimental setup to determine the K-shell photoelectric cross-section of Dy, Ta, Pt and Au atoms was implemented at the Nuclear Analytical Laboratory (LAN) of the InSTEC. Bremsstrahlung photons, produced by <sup>90</sup>Sr-<sup>90</sup>Y beta particles hitting a thin Ni converter, were used to irradiate the target under study. A HPGe detector, coupled to standard nuclear instrumentation, collected the incident and transmitted spectra. A sharp decrease in intensity at the K-shell binding energy was observed in the transmitted spectra. The photon beam divergence effects were corrected with a calibration curve calculated with Monte Carlo simulations (MCNPX 2.6). In order to establish accurately the cross section at the K-edge energy, the obtained data was processed by two methods: fitting the total cross section to a sigmoidal function, as well as the cross section branches around the K-edge to the empirical law  $\sigma = (A/E)^n$ . The Empirical Law method was introduced in this work to minimize the detector resolution effects. The results were compared with experimental and theoretical values showing the best agreement when the thinner targets were used. For the first time the photoeffect cross section at the K-edge energy for Pt is reported at first time.

**Key words:** bremsstrahlung, photoelectric effect, cross sections, Monte Carlo method, measuring instruments

## Medición de la sección eficaz de fotoefecto y de la energía del borde de absorción K de los átomos Dy, Ta, Pt y Au utilizando radiación de frenado

### Resumen

Se determina la sección eficaz fotoeléctrica de la capa K de los átomos Dy, Ta, Pt y Au en un arreglo experimental desarrollado en el Laboratorio Analítico Nuclear del InSTEC. Los blancos bajo estudio se irradiaron con fotones de frenado producidos en un radiador de Ni por las partículas beta emitidas por una fuente de <sup>90</sup>Sr-<sup>90</sup>Y. Los espectros incidentes y de transmisión se colectaron en un detector de germanio hiperpuro, acoplado a su instrumentación nuclear estándar. En los espectros de transmisión se observó un decrecimiento agudo de la intensidad correspondiente a la energía del borde K. Los efectos de interacciones múltiples del haz fotónico en las láminas blanco se corrigieron a través de una curva de calibración calculada mediante simulaciones Monte Carlo (MCNPX 2.6). Con vistas a garantizar la mejor precisión en la determinación de la sección eficaz para la energía del borde K, los datos obtenidos se ajustaron según dos comportamientos funcionales en esta región: una sigmoide y una ley empírica del tipo  $\sigma = (A/E)^n$ . Este último método se introdujo en el trabajo y permite minimizar los efectos resolutivos. Los resultados obtenidos se compararon con valores teóricos y experimentales, mostrando mayor concordancia cuando se emplean blancos finos. Se reporta, por primera vez, la sección eficaz de fotoefecto en el borde K del platino (Pt).

**Palabras clave:** radiación de frenado, efecto fotoeléctrico, secciones eficaces, método de Monte Carlo, instrumentos de medida

## Introduction

The interaction of X-ray with matter has been extensively studied for several years owing to its application in medical physics, radiation biology, solids state physics and elemental analysis [1-3]. The interaction cross section and other related atomic parameters should be known accurately to achieve, for example, better estimations of deposited doses or lower uncertainties in absolute or semi absolute analytical X-ray Fluorescence Analysis methods. In this direction, numerous researchers have used diverse theoretical models to compile the photon cross sections and created software and databases like XCOM [4-9] for elements and compounds in the energy region from 1 keV to 100 GeV. In the low-energy region ( $E < 100$  keV), the photoelectric effect (PE) is predominant.

The most precise experimental values of K-shell PE cross sections have been obtained for low and medium Z elements with the use of synchrotron radiation [10]. Only using modern synchrotrons the measurements can be extended to high-Z elements. However, alternative methods are normally used adopting two geometrical configurations: the broad- and the narrow-beam configurations. In the first one, the intensity of the K-X ray photons emitted from the target is measured when it is excited by a monoenergetic beam of gamma source [11]. The PE CS can be determined after know the K shell fluorescence cross section, the theoretical values of fluorescence yield and the jump ratio. In the narrow beam configuration, the intensity of the transmitted photons through the target is measured at energies below and above the K edge [12]. Both methods involve the selection of a K-edge value to measure the K shell PE cross sections.

In the present work, a method described by Nayak and Badiger [13,14] was used. A new method that reduces the resolution effects and allows to obtain more accurate results was also introduced. MC simulations were carried out to design and calibrate the experimental setup. The K-shell photoelectric cross section for Dy, Ta and Au as well as the K-edge energies are measured and compared with previous data. These experimental results for Pt are reported for the first time these experimental results for Pt.

## Materials and Methods

In the experimental arrangement sketched in Figure 1, the  $\beta$  particles from a  $^{90}\text{Sr}$ - $^{90}\text{Y}$  source (60  $\mu\text{Ci}$ ), shielded by a Fe holder, hit the Ni radiator (Goodfellow foil, 44.5  $\text{mg}\cdot\text{cm}^{-2}$ ) generating Bremsstrahlung photons. This radiation, collimated by a Pb-Cd cylinder with an internal diameter of 0.6 cm, strikes the pure elemental targets of Dy ( $\text{mg}\cdot\text{cm}^{-2}$ ), Ta (207.5  $\text{mg}\cdot\text{cm}^{-2}$ ), Pt (267.6  $\text{mg}\cdot\text{cm}^{-2}$ ) or Au (94.4  $\text{mg}\cdot\text{cm}^{-2}$ ). A Plexiglas cylinder (thickness 1.0 cm) was placed behind the radiator to absorb the remaining electrons.

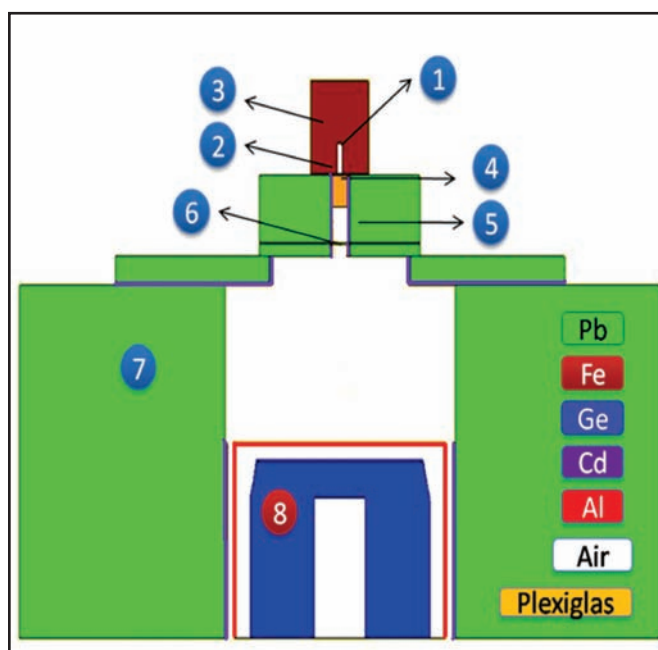


**Figure 1.** Sketch of the experimental setup showing the location of the  $^{90}\text{Sr}$ - $^{90}\text{Y}$  source (1), Ni radiator (2), source Fe holder (3), electron absorber (4), Pb-Cd collimator (5), foil target (6), Lateral Pb-Cd shielding (7) and HPGe detector (8)

A HPGe n-type detector (FWHM = 1.38 keV at 88 keV  $^{109}\text{Cd}$  line) collected the photon spectra  $I_0$  and  $I_i$  without and with the studied targets, respectively. The spectrometer parameters were fixed to measure the energy range of 20-190 keV and to assure a channel bin of 0.1 keV. The whole spectrums were recorded during a period of 11 h (Figure 2). For the transmitted spectra it is noticeable a sudden decrease in the photon intensity due to PE absorption at K-edge energy. Furthermore are visible the characteristic X rays of each target element as well as the Cd and Pb  $K_\alpha$  and  $K_\beta$  lines, constituent materials of the shield and collimation systems.

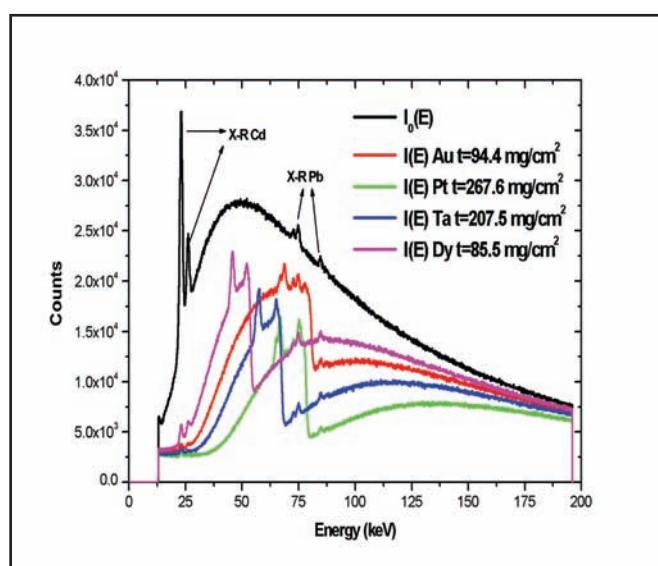


**Figure 2.** Spectra collected without ( $I_0(E)$ ) and with the targets ( $I_i(E)$ )

The photon intensity  $I_0$  at the i-channel and the intensity of the transmitted photons  $I_i$  at the same

channel were associated with the total cross section  $\sigma^i$  at the energy  $E^i$  by equation (1), where  $t$  and  $A$  are the target thickness and atomic mass, respectively, and  $N_0$  is the Avogadro number.

$$\sigma^i(E^i) = \frac{A}{N_0 t} \ln \left( \frac{I_0^i}{I^i} \right) \quad (1)$$

A parallel beam, as rigorously is required to apply the Eq. 1, is not fulfilled by our experimental arrangement. In this extent, a recalibration procedure was carried out with Monte Carlo simulations. The experimental setup details (dimensions, materials and configuration) were specified in the MCNPX input file, and two primary sources of photon beams, either parallel or with similar features to the real one, are studied. The ratio  $P(E)$  between the cross sections  $\sigma_{par}^{MC}(E)$  and  $\sigma_{real}^{MC}(E)$ , calculated for both beams, was used as a correction parameter:

$$P(E) = \frac{\sigma_{par}^{MC}(E)}{\sigma_{real}^{MC}(E)} \quad (2)$$

Several elements (W, Re, Ir, Pb and Bi) were used to simulate the measurement geometry for thickness similar to Dy and Au foils and to Ta and Pt foils, as detailed in Figure 3. Material independent growing behavior was observed and a straight line was fitted for the  $P(E)$  in all cases. From these results Eq. (3) or Eq (4), were assumed as correction parameters corresponding to the Tungsten target simulations, which shows the best reduced chi square ( $\chi_v^2$ ) statistic (0.88 and 0.92 with  $\nu = 58$  and  $\nu = 64$  degrees of freedom respectively). Both fit pass the goodness  $\chi_v^2$  test with a coverage factor  $k = 2$ . The relative uncertainty in the fitted parameters was below 1.5% in all cases.

$$P_1(E) = 1.0384 + 2.19 \cdot 10^{-3} E \quad 86 \leq t \leq 100 \text{ mg/cm}^2 \quad (3)$$

$$P_2(E) = 1.0541 + 3.62 \cdot 10^{-3} E \quad 205 \leq t \leq 264 \text{ mg/cm}^2 \quad (4)$$

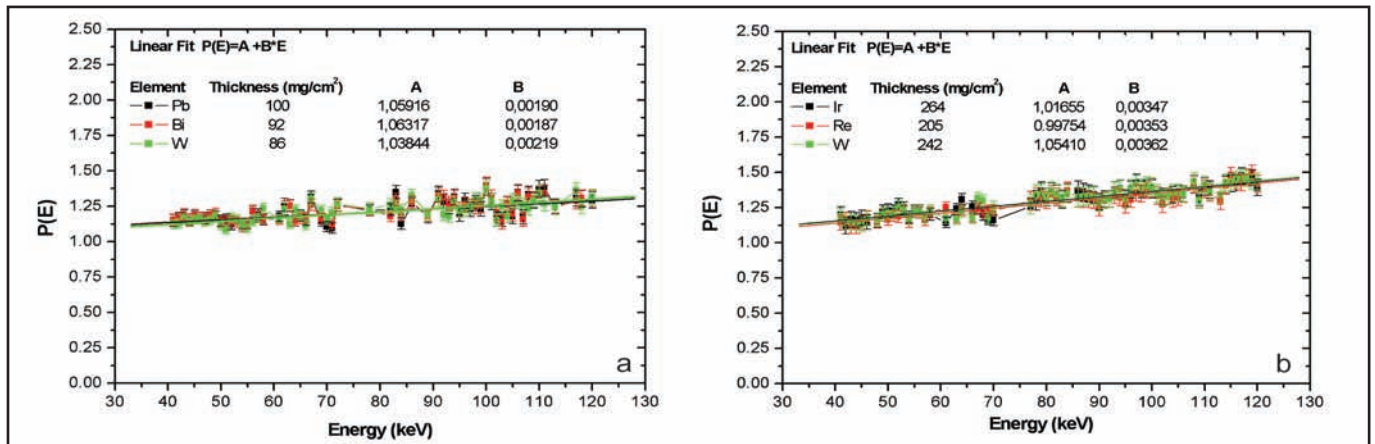


Figure 3. Ratio between the cross sections calculated with MCNPX using a parallel and “real” photon beam. Thickness interval: (a) –  $86 \leq t \leq 100 \text{ mg.cm}^{-2}$ , (b) –  $205 \leq t \leq 264 \text{ mg.cm}^{-2}$

Finally, the corrected experimental cross section (Figure 4) was calculated as:

$$\sigma_c^i(E^i) = P_{1,2}(E^i) \sigma^i(E^i) \quad (5)$$

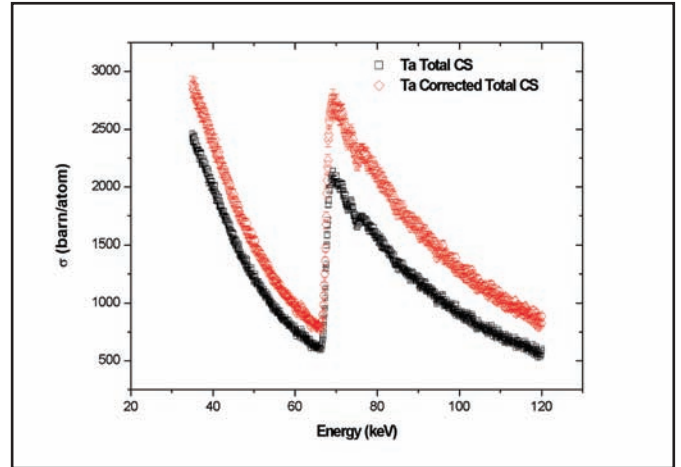
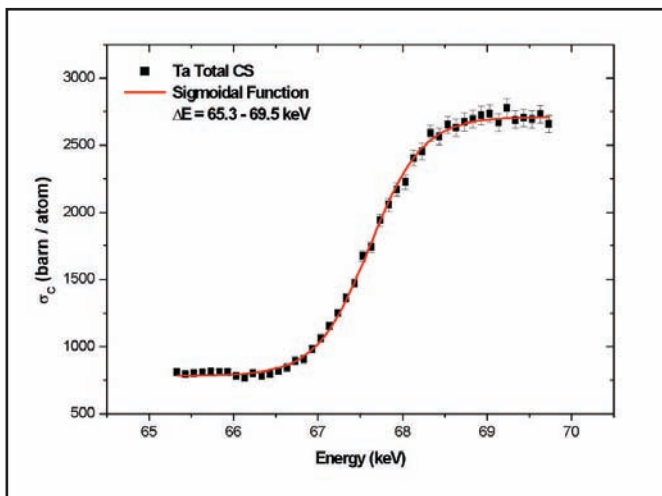


Figure 4. Total PE cross section directly measured and corrected for Ta target as function of photon energy

In order to find the cross section below ( $\tau_-$ ) and above ( $\tau_+$ ) the edge and also to determine the precise value of the K-shell binding energy  $E_k$ , two methods were used. The first one takes into account the constant behavior for both branches of the cross section, observed around the K- edge (Figure 5). Then, the experimental points were fitted to a sigmoidal function given by the Eq.6 in a range  $\Delta E \approx 4 \text{ keV}$  [13,14].

$$\sigma(E) = \frac{\tau_+ - \tau_-}{1 + \exp\left(\frac{E - E_k}{dE}\right)} + \tau_- \quad (6)$$

The difference between the  $\tau_+$  and  $\tau_-$  fitted values were considered as the experimental K shell PE cross section. Also, the first derivate of this function gives a Gaussian distribution (Figure 6), whose maximum corresponds to the  $E_k$  value (inflection point of the sigmoidal function). The  $E_k$  value was identified as the energy of the K-absorption edge.



**Figure 5.** Total PE cross section for Ta target around the K-edge and fitted sigmoidal function

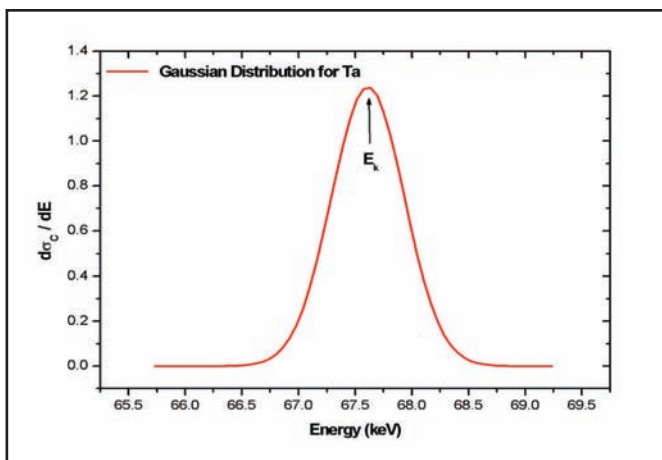


**Figure 6.** First derivate of the fitted sigmoidal function for Ta

The sudden cross section increase of the PE in the K-edge is smoothed due to the limited detector resolution, which leaves to underestimate the PE cross section data. A better energy resolution entails a sharpness measured edge, and then a higher PE cross section value was calculated by the subtraction of the cross section branches. Therefore, the application of this method is restricted by the detector resolution. An alternative procedure, consisting into fitting both cross section branches to an empirical law like Eq. 7 was carried out [15]. The parameters  $B$  and  $n$  were determined using the logarithmic regression given by Eq. 8. The K shell PE cross section was determined evaluating at the  $E_k$  energy (obtained by the first method) the empirical laws in both branches (Figure 7).

$$\sigma(E) = \left( \frac{B}{E} \right)^n \quad (7)$$

$$\ln(\sigma) = B' - n \ln(E) \quad (8)$$

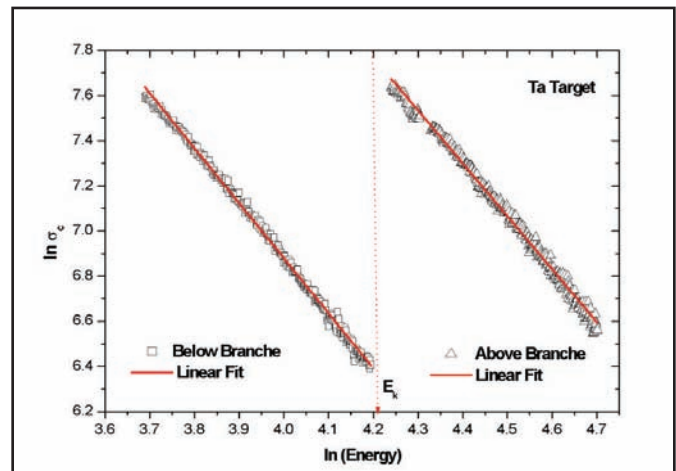


**Figure 7.** Below and above branches linear fitted function for out of K-edge region

## Results and Discussion

The measured K-edge energies are shown in Table 1. A systematic difference ( $\sim 200$  eV) is observed in all cases, except for Au, where the closest results to the compared data are achieved. These discrepancies are mainly conditioned by the detector resolution. Some  $K_\beta$  characteristics X-rays emitted by the atom targets are detected in the energy region corresponding to the steep fall. Therefore, a smooth increase is observed for the cross section at the edge zone ( $\Delta E \sim 2$  keV) and the  $E_k$  value could be overestimated.

**Table 1.** Measured K-edge energies and comparison with reported theoretical data

CRM	Method	
	Sigmoidal Fit	Other Reports
Dy	$53.914 \pm 0.004$	53.790 [4] 53.790 [7] 53.789 [12]
Ta	$67.608 \pm 0.003$	67.420 [7] 67.416 [17] 57.514 [13]
Pt	$78.609 \pm 0.003$	78.390 [4] 78.390 [7] 78.395 [17]
Au	$80.751 \pm 0.004$	80.720 [7] 80.725 [17] 80.780 [13]

On the other hand, the use of a continuous Bremsstrahlung photon spectra and the fact of fitting the experimental points to a sigmoidal function, makes feasible to report the K-shell binding energy with an accuracy of less than  $\pm 10$  eV.

The PE cross section values obtained by using the two methods earlier described are summarized in Table 2. Discrepancies within 10-20% are observed between them. The Sigmoidal Fit method underestimates the PE cross sections, similarly to the K-shell binding energy determination, while the introduced Empirical Law Fit method shows a better agreement with the previously data reported. The comparison with theoretical data reported by Berger [7] show deviations below 5% for the thinner foils (Dy, Au).

**Table 2.** Measured photoelectric cross sections (in barn) and comparison with reported data

Element	Sigmoidal Fit	Empirical Law Fit	Other reports	Discrepancy (%)	
				Sigmoidal Fit	Empirical Law Fit
Dy	3178 ± 18	3517 ± 12	3620 [12]	-12	-3
			3580 [7]	-11	-2
			4059 [4]	-21	-13
Ta	1988 ± 27	2436 ± 34	2747 [7]	-28	-11
			2782 [4]	-29	-12
			2612[13]	-24-	-7
			2465 [16]	-19	-1
Pt	1811 ± 18	2094 ± 21	2326 [7]	-22	-10
			2549 [4]	-29	-18
Au	1998 ± 25	2208 ± 24	2278 [7]	-12	-3
			2270 [4]	-12	-3
			1830 [13]	9	20

## Conclusions

An experimental arrangement was designed for the determination of photoelectric cross section and the K-edge energy. In order to consider the multiple scattering effects on the target, a correction factor for the measurements was introduced by means of Monte Carlo simulations. The photoeffect cross section at the K-edge energy for Pt is reported for the first time.

The comparison between the obtained photoeffect cross sections for Dy, Ta and Au and worldwide reported data shows that: 1) the sigmoidal fit method is not recommended as it is strongly dependent on the detector energy resolution, (it is not possible a correct characterization of the K-edge zone); 2) the introduced Empirical Law method achieves better results for the same experimental conditions; 3) the best agreement was reached for the thinner foils: Dy and Au, where multiple scattering effects are negligible. Then, the results can be improved by the use of targets with thickness bellow 10 mg/cm<sup>2</sup> and the Empirical Law method.

## References

- [1] HUBBELL JH. Review and history of photon cross section calculation. *Phys Med Bio.* 2006; 51(13): 245-262.
- [2] HUBBELL JH. Review of photon interaction cross section data in the medical and biological context. *Phys Med Biol.* 1999; 44(1): 1-22.
- [3] GERWARD L. X-ray attenuation coefficients: Current state of knowledge and availability. *Radiat Phys Chem.* 1992; 41(4-5): 783-789.
- [4] VEIGELE WJ. Photon Cross Section from 0.1 keV to 1 MeV for Elements Z=1 to Z=94. *Atomic. Data Tables.* 1973; 5: 51-111.
- [5] SCOFIELD JH. Theoretical photoionization cross sections from 1 keV to 1500 keV. UCRL-51326. California: Lawrence Livermore Laboratory, 1973.
- [6] CHANTLER CT. Theoretical Form Factor, Attenuation and Scattering Tabulation for Z=1-92 from E=1-10 eV to E=0.4-1.0 MeV. *J Phys Chem Ref Data.* 1995; 24: 71-94.
- [7] BERGER MJ, HUBBELL JH. XCOM: Photon Cross Sections on a Personal Computer. NBSIR 87-3597. Gaithersburg: National Bureau of Standards (former name of NIST), 1987.
- [8] BERGER MJ, HUBBELL JH. XCOM: Photon Cross Sections Database, Web Version 1.2. Gaithersburg MD 20899, USA: National Institute of Standards and Technology. 1999. Available <http://physics.nist.gov/xcom>. Originally published as NBSIR 87-3597. XCOM: Photon Cross Sections on a Personal Computer.
- [9] GERWARD L. X-ray absorption in matter. *Reengineering XCOM. Rad Phys Chem,* 2001; 60: 23-45.
- [10] KARABULUT A, GUROL A, BUDAK G, POLAT R. Measurements of L subshell and total L shell photoeffect cross-sections for some elements in 72 ≤ Z ≤ 92. *Eur Phys J. D.* 2002; 21(1): 57-61.
- [11] CHANTLER CT, TRAN CQ, BARNEA Z, et. al. Measurement of x-ray mass attenuation coefficient of copper using 8.85 – 20 keV synchrotron radiation. *Phys Rev A.* 2001; 64(6): 062506-062513.
- [12] MALLIKARJUNA ML, APPAJI GORDA SB, GOWDA R, UMESH TK. Studies on photon interaction around the K-edge of some rare-earth elements. *Rad Phys Chem.* 2002; 65(3): 217-223.
- [13] NAYAK SV, BADIGER NM. Measurement of K-shell photoelectric absorption parameters of Hf, Ta, Au, and Pb by an alternative method using a weak β-particle source. *Phys Rev A.* 2006; 73(3): 032707.
- [14] NAYAK SV, BADIGER NM. A novel method for measuring K-shell photoelectric parameters of high-Z elements. *J Phys B.* 2006; 39(12): 2893.
- [15] JAMES RW. *The Optical Principles of Diffraction of X-rays.* London: Bell & Sons, 1948.
- [16] HOSUR SB, BADIGER NM, NAIK LR. Determination of K-shell oscillator strengths and the imaginary form factors of atoms using a weak beta source. *J Phys B.* 2008; 41(9): 095003.
- [17] SANCHEZ DEL RIO M, BRUNETTI A, GOLOSIO B, et. al. XRAYLIB tables (X-ray fluorescence cross-section). Calculation using XRAYLIB 2.3. European Synchrotron Radiation Facility and University of Sassari, 2003.

Recibido: 30 de abril de 2013

Aceptado: 24 de octubre de 2013